OSIRIS-REx Orbit Trim Strategy

Daniel R. Wibben[1], Andrew Levine[2], James V. McAdams[2], and Peter G. Antreasian[3]
KinetX, Inc., Simi Valley, CA

Samantha Rieger[2], Kenneth M. Getzandanner[4], and Michael C. Moreau[5]
NASA Goddard Space Flight Center Code 595, Greenbelt, MD

Dante S. Lauretta[6]
University of Arizona, Tucson, AZ 85705

One of the more challenging aspects of the trajectory design for the OSIRIS-REx (Origins, Spectral Interpretation, Resource Identification, and Security-Regolith Explorer) mission at asteroid Bennu was maneuvering while in orbit. The orbital dynamics were highly perturbed by various sources, most notably solar radiation pressure, which degraded accuracy of long term predictions of the spacecraft's location in orbit. Generally, the Navigation team had to solve three separate issues: correcting a perturbed orbit, changing to a different orbit, or phasing the orbit to place the spacecraft at a specific location at a specific time. The team composed a common framework using up to two maneuvers that could solve all of these problems using an identical schedule that allowed for consistent planning long before the final trajectory could be designed. This orbit trim strategy was successfully used for the first time in the Orbital B phase of the mission to maximize the duration of usable observing geometry in a time-variable orbit with strict operational limits. It was used an additional 3 times throughout the mission to adjust and/or change the orbit, most notably altering the orbit in the weeks prior to the successful Touch-And-Go (TAG) sample collection attempt. This same strategy was used to phase the orbit a total 10 times in preparation for each of the science sorties over potential sample sites, the TAG Rehearsals, and TAG. The trim strategy was demonstrated to be robust and performed exceptionally well in all aspects, which proved critical to a successful sample collection.

I. Introduction

NASA's Origins, Spectral Interpretation, Resource Identification, and Security—Regolith Explorer (OSIRIS—REx) asteroid sample return mission [1] arrived at target near-Earth asteroid Bennu [2] in late 2018, and it successfully first entered orbit around the asteroid on December 31, 2018. [3] After two months in the 1.8-km semi-major axis Orbital A, the spacecraft departed orbit to perform 14 hyperbolic flybys to enable comprehensive imaging of Bennu's surface during the Detailed Survey. [4] Following these flybys, the spacecraft re-entered orbit at 925-m radius for the Orbital B mission phase in the summer of 2019. During the Orbital B phase, the spacecraft continued LIDAR asteroid surface mapping at higher resolutions than any data set obtained previously. [1,5,6] The ultimate goal of this phase was to create high-resolution, full-surface asteroid topographic maps, which were among the most important data products necessary for sample collection target selection. [7] Throughout the remainder of

[1] OSIRIS-REx Trajectory and Maneuver Design Lead
[2] OSIRIS-REx Trajectory and Maneuver Analyst
[3] OSIRIS-REx Navigation Team Chief
[4] OSIRIS-REx Flight Dynamics System Lead
[5] OSIRIS-REx Deputy Project Manager
[6] OSIRIS-REx Principal Investigator

Bennu proximity operations, the spacecraft spent a majority of time in various orbits because they required less overall effort from the team when compared to keeping the spacecraft in a hyperbolic trajectory. Following a successful sample collection attempt in October 2020 [8], the spacecraft departed the asteroid in May 2021 with the stowed surface material sample, and Earth return is scheduled in September 2023.

Due to Bennu's small (500-m diameter) size, spacecraft motion around the asteroid is highly perturbed by solar radiation pressure (SRP) effects. This presents a significant challenge in orbit design, because a closed orbit will evolve over time, creating potentially unstable conditions in which the spacecraft could either escape asteroid orbit or impact the asteroid's surface. [9] As detailed in previous works, the first orbit achieved by OSIRIS-REx (Orbital A) utilized a frozen orbit design with a 1.8-km semi-major axis. [3,10] This design minimized the impact of SRP perturbations on the orbital elements over time, providing a long-term stable orbit that required minimal maintenance. [10] This phase was so successful that the frozen orbit design was utilized several other times throughout the mission. First in the Orbital C phase (late Summer 2019), which was added to the mission plan to essentially re-create the same conditions as Orbital A for further investigation of the particle ejections from Bennu's surface that were discovered just after the initial orbit insertion in January 2019. [11] The frozen orbit concept was again used as the 'safe-home orbit' throughout the Reconnaissance and Sample Collection mission phases, as it provided long-term stability for the spacecraft, with the lower level of operations team effort enabling time to focus on the planning and development of upcoming spacecraft activities such as reconnaissance sorties over potential sample sites [12], Touch-And-Go (TAG) sample collection rehearsals, and TAG [8]. While each of these phases utilized the same base concept of an orbit that is frozen to offset SRP perturbations and prevents significant evolution in its orbital parameters over time, each orbit had unique requirements and thus was sized and/or oriented differently. As an example, the Orbital A design featured a semi-major axis of 1.8-km and longitude of ascending node of 90 deg (in the Sun Anti-Momentum (SAM) frame) while the orbit prior to TAG had a semi-major axis of 0.9-km and a longitude of ascending node of 270 deg (i.e. the orbits rotated in opposite directions and swapped periapse/apoapse locations relative to the asteroid surface). Thus, a general methodology was required in order to transition the spacecraft between these various orbits. In addition, due to maneuver execution or orbit determination prediction errors at orbit insertion, the desired frozen conditions may not have been achieved exactly, thus orbit maintenance may have been required to correct for these errors.

In contrast to the frozen orbits used in other mission phases, the 925-m semi-major axis Orbital B could not utilize a frozen orbit as some of the unique properties of this orbit design were detrimental to acquisition of global science data during this phase. Most importantly, frozen orbits require specific (non-zero) eccentricities, which conflict with the requirement to maintain a near-constant distance to the surface for consistent LIDAR ranging data collection. Terminator frozen orbits are designed to minimize orbital element evolution and subsequently would hold the locations of periapse and apoapse constant relative to the asteroid surface. In such an orbit, these would always remain near the poles of the asteroid, thereby providing data with higher resolution over one pole than over the other. The design of the Orbital B trajectory instead required an orbit that evolved in a controlled manner over the six-week observation period in order to provide full, even coverage of the asteroid's surface. In addition, the number of orbit adjustments had to be minimized to provide more precise prediction of the spacecraft's location in orbit, which in turn maximized science return and also the probability of achieving full science coverage of Bennu’s surface. Further complicating the trajectory design, the spacecraft’s orbit plane was required to always remain within 10 degrees of the terminator (day/night) plane due to spacecraft thermal and power constraints. The initial orbit design for the Orbital B phase showed that SRP primarily perturbed the orbit by increasing the orbit eccentricity and longitude of ascending node if starting from a circular terminator orbit. Analysis demonstrated that the plane of such an orbit would exceed the specified operational constraints within approximately three weeks. With the Orbital B global mapping phase requiring at least six weeks in order to achieve global coverage, it implied that at least one trim maneuver would be necessary in order to adjust the orbit and remain within operations boundaries. While the initial and target orbits are quite different in Orbital B, the underlying problem remained the same throughout all orbital phases: a robust strategy was required in order to reliably maintain or adjust the spacecraft's orbit around Bennu whenever necessary.

Later in the mission, the Reconnaissance, TAG Rehearsals, and TAG mission phases required the spacecraft to be delivered to a specific location in orbit at a specified time, which coincided with key observing geometry for the potential sample sites. Given Bennu’s 4.3-hour rotation period and the strict sequence of events to be performed during the descent to the surface for TAG [8], the issue of phasing the spacecraft’s orbit was another problem that had to be solved in order to boost the potential for a successful sample collection.

This paper focuses on the orbit trim, transfer, and phasing burn strategy devised for OSIRIS-REx while in orbit around asteroid Bennu. The relevant coordinate system is introduced first, followed by a detailed explanation of the common strategy used for maneuvering the spacecraft while in orbit. Next, the application of this plan for correcting

the orbit in the Orbital B mission phase and just before TAG are covered. These sections will focus on how the target orbit was determined to achieve the desired conditions, and how the sequence executed. Finally, the design and performance of the phasing maneuvers to set up the spacecraft for departing orbit to execute a Reconnaissance sortie over the potential sample sites, a TAG Rehearsal, and TAG are described.

II. Coordinate Frame Definition

Prior to the encounter, the team defined a consistent Bennu-centric coordinate frame to be used which would not change as information about Bennu's shape and orientation were gathered throughout the mission. The chosen coordinate frame, named the Sun Anti-Momentum (SAM) frame, is defined solely based on Bennu's orbit around the Sun, as depicted in Figure 1. The coordinate system has its origin at Bennu's center of mass, and the *x*-axis points along the Bennu-Sun line. The *z*-axis is in the opposite direction of Bennu's heliocentric orbital angular momentum vector, and the *y*-axis completes the right-handed frame. All subsequent equations and orbital parameter definitions used in this paper are defined in this reference frame.

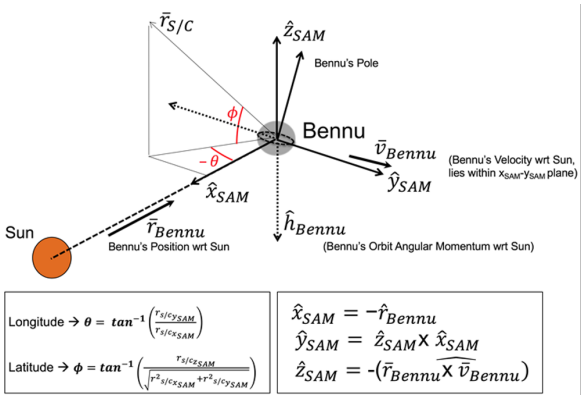

Fig. 1 Sun Anti-Momentum coordinate frame definition

Note that this rotating coordinate frame rotates about the *z*-axis with a rate of $\dot{\nu}$, Bennu's heliocentric orbit true anomaly rate, which varies based on the asteroid's distance from the Sun:

$$\dot{\nu} = \frac{\sqrt{\mu_{sun} A(1-e_B^2)}}{d^2} \tag{1}$$

where A and e_B represent the semi-major axis and eccentricity of Bennu's orbit around the Sun, μ_{sun} is the GM of the Sun, and d is the distance from the Sun to the asteroid. This frame is convenient when considering the perturbing acceleration due to SRP, which for a spherical spacecraft with constant optical properties is stated as:

$$\boldsymbol{a}_{SRP} = -\frac{(1+\rho_s)\Phi}{Bd^2}\,\hat{\boldsymbol{x}}_{SAM} \tag{2}$$

where ρ_s is the reflectance of the spacecraft, $\Phi \sim 10^8\ kg\ km^3\ s^{-2}\ m^{-2}$ is the solar pressure constant, and B is the spacecraft mass to area ratio in kg/m^2.

III. Methodology

In the original trajectory design, adjusting the spacecraft's orbit was viewed as three separate problems, each requiring their own unique solution:

1) Perform orbit maintenance, or "trim" the orbit, if it is predicted to fall outside the allowable operations regime. Ideally this could be done with a single maneuver, assuming the current and desired orbits intersect.
2) Transfer from one orbit to another. Naturally this solution would require at least two maneuvers – one to initiate the transfer and one to complete it and arrive in the desired target orbit.
3) Phase the orbit to deliver the spacecraft to a desired point at a specific time, with minimal change to the existing orbit. This was necessary for Reconnaissance sorties, the TAG Rehearsals, and TAG in order to bring the spacecraft to the orbit departure maneuver (ODM) location at the proper time.

Analysis quickly demonstrated that it was not tenable to perform orbit maintenance with a single maneuver. To do so would require very accurate predictions of the location of the spacecraft in orbit far enough in advance for maneuver design planning. Operationally, the team had a minimum turnaround time from final maneuver design to execution of approximately 24 hours, but maneuver start times had to be determined at the preliminary design, which was between 7-12 days prior to maneuver execution. Orbit determination performance showed that a data cutoff of 7 days prior to maneuver execution led to a downtrack (i.e. true anomaly) error of approximately 10 deg (1σ) [13,14], depending on orbit size, while a prediction of less than 5 deg (3σ) was necessary in order to reliably plan and design an orbit adjustment. Instead, a strategy was devised to perform orbit maintenance using a two-maneuver sequence. The first would execute at a fixed time to force the spacecraft to the desired location at the time of the second burn, which would perform the orbit change. With this strategy, it is easy to see how the three different techniques can all utilize a single solution, with minor nuances differentiating each scenario. Trim and transfer sequences look identical from a scheduling perspective and only differ in the final target, while a phasing maneuver is accomplished using only the first burn in the sequence.

Figure 2 shows an example of the general orbit trim maneuver schedule utilized throughout Bennu proximity operations. The first maneuver is executed at a fixed time on Day 1. Optical Navigation (OpNav) images are downlinked the following day to refine the orbit and thereby help reconstruct the maneuver, which is then used to revise the design of the second maneuver, to be uplinked a few hours before maneuver execution on Day 3. Execution errors were accounted for by building in a short time window within which the second maneuver could be performed, which was nominally centered at 54 hours after the first burn. This timing was chosen to allow enough time to perform all the activities necessary to uplink a revised design of the second burn prior to execution. Additionally, the time between maneuvers was required to be large enough compared to the orbital period such that any true anomaly could be reached. Early on, the allowable time window for the second burn was ±3 hours, but as the team gained confidence and improved modeling, the window decreased to ±2 hours. The actual maneuver start time was determined when the late update was performed in the 24 hours between High Gain Antenna (HGA) passes on days 2 and 3. The final maneuver execution time was then uplinked to the spacecraft along with the final maneuver parameters in the HGA pass just prior to maneuver execution.

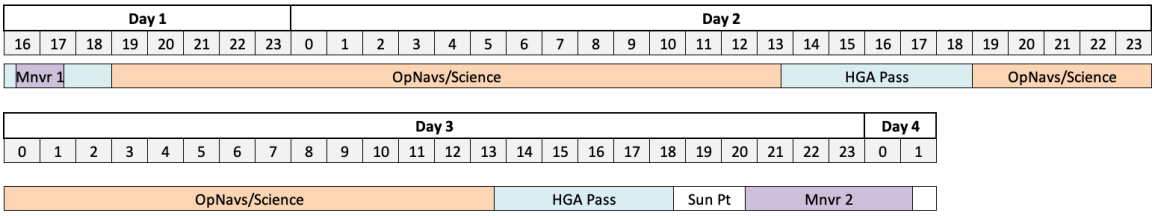

Fig. 2 Sample Trim Maneuver Schedule

The mission plan accounted for up to 30 potential orbit trims; one after each of the 10 orbit insertions that were performed, and periodically while remaining in orbit. Exceptional navigation performance meant most of these were not required. This orbit-trim strategy was used in full only 4 times throughout the mission, for various purposes:

1) Orbital B trim to correct orbit evolution and provide 6 weeks of maneuver-free propagation for LIDAR data collection (detailed in a later section)
2) Transfer from the 925 m semi-major axis Orbital B to the 1.75 km semi-major axis, frozen Orbital C
3) Orbit trim prior to the first TAG Rehearsal to correct the orbit plane and reduce orbit size by 150 m, both of which were necessary to place the Rehearsal orbit departure maneuver (ODM) at the correct location
4) Pre-TAG trim to correct orbit plane (detailed in a later section)

The maneuver designs and performance for each of these orbit trims are summarized in Table 1. Outside of the transfer to Orbital C, which required larger maneuver magnitudes due to the larger change in orbit sizes, the ΔV of these maneuvers ranged between 0.45 and 1.855 cm/s. The performance of maneuvers of this small size is commendable, which generally performed below 1σ of the *a-priori* error. The execution times listed in Table 1 also show the largest time shift for the second maneuver in the trim was seen with the transfer to Orbital C, which at just under 37 minutes was still well within the allotted window of ±3 hours.

Table 1 – Trim maneuver performance

Maneuver	Date (SCET-UTC)	Parameter	Nominal Value	Estimated Value	*A-priori* Sigma	Estimated Sigma	Correction	Correction / *A-priori*
Orbital B Trim 1	25-Jun-2019 17:00:00	ΔV, cm/s	1.53900	1.55500	0.05140	0.00100	0.01600	0.31128
		RA, deg	22.92794	22.58749	1.14800	0.06936	-0.34045	-0.29656
		Dec, deg	-63.57659	-63.78764	0.51080	0.03344	-0.21104	-0.41316
Orbital B Trim 2	27-Jun-2019 23:00:00	ΔV, cm/s	1.85500	1.88600	0.01589	0.00100	0.03100	1.95091
		RA, deg	231.36705	231.23981	0.31280	0.02708	-0.12725	-0.40681
		Dec, deg	21.17453	21.07189	0.29160	0.02996	-0.10264	-0.35199
Orbital C Transfer 1	06-Aug-2019 17:00:00	ΔV, cm/s	2.27300	2.30000	0.01630	0.00400	0.02600	1.59509
		RA, deg	170.24005	170.74321	0.68140	0.14760	0.50316	0.73842
		Dec, deg	-64.66049	-64.84307	0.29160	0.08626	-0.18258	-0.62613
Orbital C Transfer 2	08-Aug-2019 23:36:47	ΔV, cm/s	3.04600	3.07400	0.01731	0.00100	0.02800	1.61756
		RA, deg	296.53362	296.12944	0.58190	0.03903	-0.40418	-0.69459
		Dec, deg	59.92155	59.83994	0.29160	0.02761	-0.08162	-0.27990
Rehearsal Trim 1	10-Mar-2020 17:00:00	ΔV, cm/s	1.36500	1.34600	0.04557	0.00084	-0.01860	-0.40813
		RA, deg	168.16690	167.95347	0.94310	0.07451	-0.21343	-0.22631
		Dec, deg	-57.10625	-57.10175	0.51220	0.02443	0.00450	0.00879
Rehearsal Trim 2	12-Mar-2020 23:07:20	ΔV, cm/s	1.27500	1.30100	0.01543	0.00148	0.02590	1.67846
		RA, deg	345.56729	346.27478	0.40050	0.07453	0.70748	1.76649
		Dec, deg	43.26597	43.23483	0.29160	0.04416	-0.03114	-0.10679
TAG Trim 1	06-Oct-2020 17:00:00	ΔV, cm/s	1.04950	1.06590	0.03508	0.00106	0.01630	0.46466
		RA, deg	273.00725	272.85397	0.52950	0.06915	-0.15327	-0.28946
		Dec, deg	-13.03036	-13.10631	0.51580	0.02520	-0.07595	-0.14725
TAG Trim 2	08-Oct-2020 22:50:00	ΔV, cm/s	0.45080	0.44200	0.01526	0.00102	-0.00880	-0.57664
		RA, deg	117.13733	117.19878	0.53890	0.14770	0.06144	0.11401
		Dec, deg	4.88991	4.43753	0.53690	0.15010	-0.45238	-0.84258

Ten phasing maneuvers, which utilized only the first burn in the sequence, were required in support of the Reconnaissance sorties, both TAG Rehearsals, and TAG. The two rehearsals, known colloquially as Checkpoint (CP) Rehearsal and Matchpoint (MP) Rehearsal, are named based on how far into the TAG sequence they progressed before backing away from the asteroid. Analysis was performed prior to arrival at Bennu on these small maneuvers in order to determine how many phasing maneuvers would be required and what schedule would satisfy delivery requirements for TAG. The results showed that up to two phasing maneuvers would be required for each orbit departure, and these could be performed on a reasonable schedule of 7 days and 3 days prior to ODM. Maneuver performance for each phasing burn is shown in Table 2, with ΔV results notably printed in units of mm/s. These maneuvers were the smallest performed in the mission, with the smallest being the second phasing burn for CP Rehearsal with a ΔV of just 0.09 mm/s. Other than the CP Rehearsal 1 phasing maneuver, which will be discussed later, all maneuvers performed near or below 1σ of the *a-priori* execution error, greatly outperforming pre-encounter assumptions.

The following sections provide examples of how this strategy was used throughout the mission, with specifics provided in each section on how the target orbit was determined, and how the sequence performed when executed.

IV. Orbital B Design and Results

The non-frozen nature of the Orbital B phase required a unique approach to maintaining the orbit. As mentioned previously, science required at least 6 weeks without any maneuvers to achieve full coverage. Due to the evolution of the longitude of ascending node of the orbit due to SRP, an initially circular orbit would naturally evolve outside the allowable regime of 10 deg from the terminator plane after approximately 3 weeks. To maximize the time between orbit trims, the design instead had to target an orbit that would evolve to become circular after several weeks, such as the example shown in Figure 3. The desired target after an orbit trim in this case is the orbital parameters corresponding to the far left of the plot. Determining this initial state required analysis of the equations of motion and evaluation of the impact of various perturbing accelerations on the spacecraft in a sub-1 km sized orbit.

Table 2 – Phasing maneuver performance

Phasing Maneuver	Date (SCET-UTC)	Parameter	Nominal Value	Estimated Value	*A-priori* Sigma	Estimated Sigma	Correction	Correction / *A-priori*
Nightingale Medium Sortie	14-Jan-2020 17:00:00	ΔV, mm/s	3.75000	3.72000	0.12772	0.00509	-0.02600	-0.20358
		RA, deg	252.33816	252.89001	1.30100	0.32590	0.55185	0.42417
		Dec, deg	-65.25779	-65.25039	0.54440	0.14140	0.00740	0.01359
Osprey Medium Sortie	04-Feb-2020 17:00:00	ΔV, mm/s	2.58000	2.56000	0.08988	0.00708	-0.01200	-0.13351
		RA, deg	107.57900	107.28585	0.69210	0.25620	-0.29314	-0.42355
		Dec, deg	35.32827	35.13668	0.56470	0.17550	-0.19159	-0.33928
Nightingale Low Sortie	25-Feb-2020 17:00:00	ΔV, mm/s	0.92000	0.97000	0.04059	0.00433	0.05000	1.23183
		RA, deg	6.28495	5.83535	1.91300	1.39900	-0.44960	-0.23502
		Dec, deg	-69.12537	-69.69514	0.68150	0.46410	-0.56977	-0.83605
CP Rehearsal 1	07-Apr-2020 17:00:00	ΔV, mm/s	0.47000	0.56000	0.03099	0.00485	0.08600	2.77545
		RA, deg	147.45636	146.99541	1.18100	0.85470	-0.46096	-0.39031
		Dec, deg	-43.80207	-44.92309	0.85200	0.58410	-1.12102	-1.31575
CP Rehearsal 2	11-Apr-2020 17:00:00	ΔV, mm/s	0.09000	0.11000	0.02684	0.00678	0.02500	0.93155
		RA, deg	187.40920	191.19669	2.38200	2.08200	3.78749	1.59005
		Dec, deg	9.20941	10.22642	2.35200	2.05200	1.01701	0.43240
Osprey Low Sortie 1	19-May-2020 17:00:00	ΔV, mm/s	1.43900	1.44300	0.05488	0.00615	0.00400	0.07288
		RA, deg	33.63401	33.96954	0.78270	0.36990	0.33553	0.42868
		Dec, deg	38.12241	37.08157	0.61580	0.31520	-1.04084	-1.69022
Osprey Low Sortie 2	23-May-2020 17:00:00	ΔV, mm/s	3.84000	3.80000	0.13086	0.00779	-0.04700	-0.35918
		RA, deg	291.25278	291.35355	0.62790	0.13540	0.10077	0.16049
		Dec, deg	30.08496	30.19055	0.54330	0.10960	0.10559	0.19435
MP Rehearsal	04-Aug-2020 17:00:00	ΔV, mm/s	6.24200	6.26300	0.20979	0.00717	0.02100	0.10010
		RA, deg	128.82373	130.95819	5.92600	0.90200	2.13446	0.36019
		Dec, deg	84.90107	84.72860	0.52670	0.07823	-0.17246	-0.32743
TAG 1	13-Oct-2020 17:00:00	ΔV, mm/s	1.00000	0.94400	0.04269	0.01034	-0.05600	-1.31181
		RA, deg	293.97805	294.29572	0.68030	0.43540	0.31767	0.46696
		Dec, deg	11.51396	11.76689	0.66660	0.32920	0.25294	0.37945
TAG 2	17-Oct-2020 17:00:00	ΔV, mm/s	0.49800	0.50600	0.03141	0.00782	0.00800	0.25467
		RA, deg	205.39054	203.86312	1.202	0.8803	-1.52742	-1.27073
		Dec, deg	-46.0278	-46.11693	0.8346	0.5259	-0.08913	-0.10679

On average, the semi-major axis is constant to secular perturbations. [9,10] Thus the Milankovitch orbital element representation [15] is a convenient model for the averaged equations of motion for the orbital elements. The definition of these elements is described in Eqs. (3) and (4), where $\boldsymbol{r}$ and $\boldsymbol{v}$ represent the spacecraft position and velocity, μ is the GM of the asteroid, and a is the desired semi-major axis of the orbit. The state vectors in this representation are a scaled angular momentum vector $\boldsymbol{h}$ and the eccentricity vector $\boldsymbol{e}$. The $\tilde{\boldsymbol{r}}$ notation here represents the cross-product dyadic. [15]

$$\boldsymbol{h} = \frac{1}{\sqrt{\mu a}} \tilde{\boldsymbol{r}} \cdot \boldsymbol{v} \tag{3}$$

$$\boldsymbol{e} = \frac{1}{\mu} \tilde{\boldsymbol{v}} \cdot \tilde{\boldsymbol{r}} \cdot \boldsymbol{v} - \frac{\boldsymbol{r}}{|\boldsymbol{r}|} \tag{4}$$

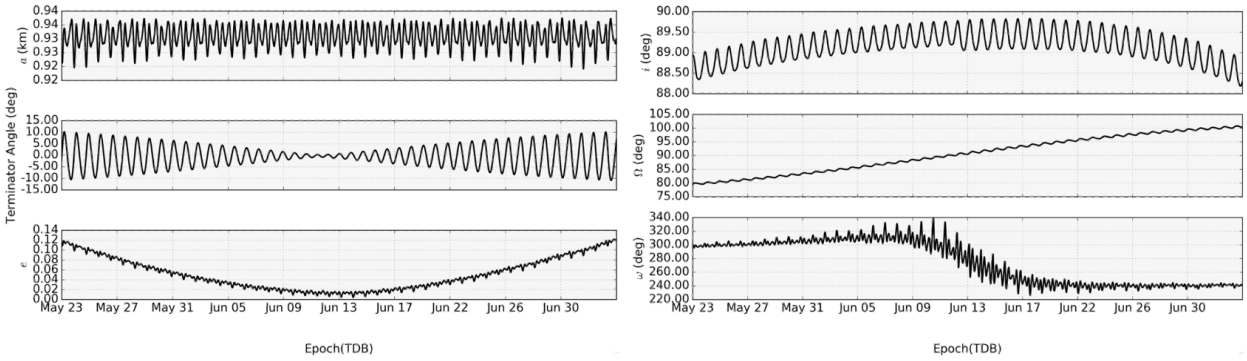

Fig. 3 Example orbit evolution in the SAM frame, reaching near-circular midway through propagation

The first-order averaged equations of motion in the rotating SAM frame can be stated in Lagrangian form as:

$$\dot{\bar{\boldsymbol{h}}} = \tilde{\bar{\boldsymbol{h}}} \cdot \frac{\partial \bar{\mathcal{R}}^*}{\partial \bar{\boldsymbol{h}}} + \tilde{\bar{\boldsymbol{e}}} \cdot \frac{\partial \bar{\mathcal{R}}^*}{\partial \bar{\boldsymbol{e}}} - \dot{\nu}\tilde{\boldsymbol{z}} \cdot \bar{\boldsymbol{h}} \tag{5}$$

$$\dot{\bar{\boldsymbol{e}}} = \tilde{\bar{\boldsymbol{h}}} \cdot \frac{\partial \bar{\mathcal{R}}^*}{\partial \bar{\boldsymbol{e}}} + \tilde{\bar{\boldsymbol{e}}} \cdot \frac{\partial \bar{\mathcal{R}}^*}{\partial \bar{\boldsymbol{h}}} - \dot{\nu}\tilde{\boldsymbol{z}} \cdot \bar{\boldsymbol{e}} \tag{6}$$

where $\bar{\mathcal{R}}^* = \bar{\mathcal{R}}(\bar{h}, \bar{e})/\sqrt{\mu a}$ is the scaled, averaged perturbing function, and is the sum of the contributions of each individual perturbing force being considered. While these equations are over-determined (the 6 state components only translate back to 4 orbital elements), this form is convenient for describing the changes in the spacecraft orbit over time. Note that these equations admit two integrals of motion that must be maintained to provide physically meaningful solutions: $\bar{\boldsymbol{h}} \cdot \bar{\boldsymbol{e}} = 0$ and $\bar{\boldsymbol{h}} \cdot \bar{\boldsymbol{h}} + \bar{\boldsymbol{e}} \cdot \bar{\boldsymbol{e}} = 1$.

As mentioned previously, the primary perturbing acceleration in the environment around Bennu is SRP, which provides a known averaged perturbing potential function [10,15], as expressed in Eq. (7). In addition, the Orbital B regime (semi-major axis of 925 m) is close enough to the asteroid that primary oblateness terms, specifically $J2$ and $J3$, are significant and also need to be considered. Taking the partial derivatives of Eq. (7) with respect to $\bar{\boldsymbol{h}}$ and $\bar{\boldsymbol{e}}$ and substituting for these in Eqs. (5) and (6), one can find that considering only SRP will manifest itself purely in evolution of e and Ω, which does not entirely coincide with the full fidelity propagation seen in Fig. 3. Thus, the averaged perturbing function for both harmonic terms were included as expressed in Eqs. (8) and (9).

$$\bar{\mathcal{R}}^*_{srp} = \frac{3a_{SRP}}{2}\sqrt{\frac{a}{\mu}}\hat{\boldsymbol{x}}_{SAM} \cdot \boldsymbol{e} \tag{7}$$

$$\bar{\mathcal{R}}^*_{J2} = -\frac{nJ_2R^2}{4a^2h^3}\left[1 - 3\left(\hat{\boldsymbol{p}} \cdot \hat{\boldsymbol{h}}\right)^2\right] \tag{8}$$

$$\bar{\mathcal{R}}^*_{J3} = -\frac{3nJ_3R^3}{8a^3h^5}(\boldsymbol{e} \cdot \hat{\boldsymbol{p}})\left[1 - 5\left(\hat{\boldsymbol{p}} \cdot \hat{\boldsymbol{h}}\right)^2\right] \tag{9}$$

Here J_2 and J_3 are the spherical harmonic coefficients, R is the mean equatorial radius, n is the mean motion of the spacecraft, and $\hat{\boldsymbol{p}}$ is aligned with the asteroid's rotation pole. The partial derivatives can be computed from these expressions, and the sum $\bar{\mathcal{R}}^* = \bar{\mathcal{R}}^*_{SRP} + \bar{\mathcal{R}}^*_{J2} + \bar{\mathcal{R}}^*_{J3}$ can be put in Eqs. (5) and (6). The full partial derivatives are expressed in Eqs. (10) and (11). The resulting equations of motion can then be back-propagated from an initially circular orbit with the specified semi-major axis until the 10-degree from terminator constraint is reached in order to find the initial conditions that maximize the time spent without requiring another trim.

$$\frac{\partial \bar{\mathcal{R}}^*}{\partial \bar{\boldsymbol{h}}} = -\frac{3nJ_2R^2}{4a^2h^5}\left[\left(1 - \frac{5}{h^2}(\hat{\boldsymbol{p}} \cdot \boldsymbol{h})^2\right)\boldsymbol{h} + 2(\hat{\boldsymbol{p}} \cdot \boldsymbol{h})\hat{\boldsymbol{p}}\right] - \frac{15nJ_3R^3}{8a^3h^7}(\boldsymbol{e} \cdot \hat{\boldsymbol{p}})\left[\left(1 - \frac{7}{h^2}(\hat{\boldsymbol{p}} \cdot \boldsymbol{h})^2\right)\boldsymbol{h} + 2(\hat{\boldsymbol{p}} \cdot \boldsymbol{h})\hat{\boldsymbol{p}}\right] \tag{10}$$

$$\frac{\partial \bar{\mathcal{R}}^*}{\partial \bar{\boldsymbol{e}}} = \frac{3a_{srp}}{2}\sqrt{\frac{a}{\mu}}\hat{\boldsymbol{x}}_{SAM} + \frac{3nJ_3R^3}{8a^3h^5}\left(\hat{\boldsymbol{p}} \cdot \hat{\boldsymbol{h}}\right)^2\hat{\boldsymbol{p}} \tag{11}$$

To this point, determining the true anomaly target (i.e., the location in the final orbit to perform the second trim maneuver, and the target of the first) has not been discussed and is the only remaining free parameter. The location at which to perform the second trim was determined after all other orbital elements were set, and was typically optimized to find the location in orbit which minimized delta-V (ΔV) for the entire transfer. Other considerations were also made, such as the size and orientation of the transfer orbit between the two trim maneuvers, and sizing the ΔV of the first maneuver such that it could be executed on the smallest thruster set on the spacecraft (0.08 N).

Due to the complexity of targeting an orbit with the exact parameters right at orbit insertion, and the possibility that maneuver execution or OD prediction errors could place the spacecraft in an entirely different orbit that did not evolve in the desired manner, the team selected to insert directly to a circular orbit at the start of the Orbital B phase. A trim would be performed to place the spacecraft in an orbit similar to that shown in Fig. 3 using the methodology described above after two weeks. After the trim was completed, science data collection would begin until the orbit needed adjustment again after 6 weeks, at which point the mission transitioned up to a larger, frozen orbit for the Orbital C phase. The targeted and achieved orbital elements for the Orbital B insertion and the trim are specified in Table 3, and the maneuver designs necessary to complete this trim are included in Table 1. Note that the trim has two sets of target states; the initial target corresponds to the targeted orbit prior to execution of the first maneuver in the trim sequence, while the final is an update made between the two trim maneuvers due to the original target no longer being achievable after errors in execution are realized. For both the orbit insertion and trim, the achieved values are the reconstructed trajectory parameters after maneuver execution is completed.

Table 3 – Orbital B Targeted and Achieved Parameters

	Orbital B Insertion		Trim Design			
	Target	**Achieved**	**Pre-Trim Orbit**	**Initial Target**	**Final Target**	**Achieved**
a, m	925.00	919.05	923.26	930.38	918.67	921.17
e	0.00	0.02	0.04	0.08	0.09	0.10
i, deg	90.00	90.51	89.63	89.91	90.09	89.94
Ω, deg	90.00	90.06	95.78	82.00	82.06	81.64
ω, deg	270.00	165.16	248.26	273.95	274.15	273.11
θ, deg	0.00	109.45	326.18	180.00	180.23	180.32

The as-flown orbital elements for Orbital B are shown in Fig. 4. The start and end times of the trim are marked with the vertical lines, which clearly placed the spacecraft in a smaller, more eccentric orbit for the 54 hours in between trim maneuvers. The semi-major axis is otherwise constant on average throughout the period as expected, though the observed small jumps in orbit size are due to spacecraft reaction wheel desaturation maneuvers (desats). The terminator angle clearly shows that the 10 deg constraint was satisfied at all times throughout the mission phase and the eccentricity was exceptionally low for a large portion of time after the trim burn was performed. As a result of this unique design and successful execution, no additional trims were necessary and all required LIDAR was collected, which provided the high-resolution topography data necessary to support sample site selection.

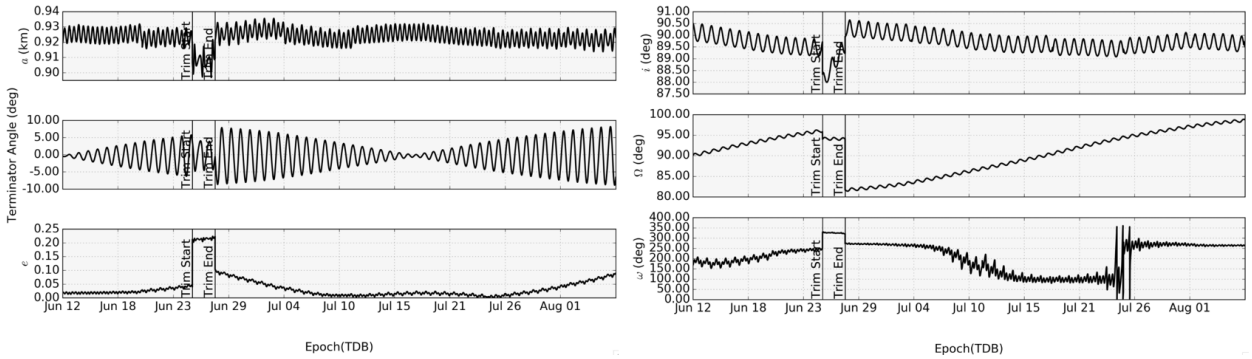

Fig. 4 As-flown Orbital B orbital parameters in the SAM frame

V. TAG Orbit Trim Results

Other than Orbital B, all other orbital mission phases used the frozen orbit concept, and so determining the target orbital elements was much more straightforward. In this case there were only three independent variables to be set by the designer in order to determine the target orbit: semi-major axis, the direction of rotation (clockwise or

counterclockwise when viewed from the Sun), and the true anomaly at which to perform the second trim maneuver. The target elements for a frozen orbit are summarized in Table 4, where the eccentricity is calculated based on the desired orbit size, and spacecraft and asteroid parameters.

Table 4 – General Frozen Orbit Elements

Parameter	Value
a, m	Set by user
e	See Eq. (18) in [10]
i, deg	90
Ω, deg	± 90 (clockwise vs counterclockwise)
ω, deg	∓ 90 (clockwise vs counterclockwise)

In the case of TAG, the orbit size needed to be such that the spacecraft was at an orbital radius of 1000 ± 50 m (3σ) at the ODM (geocentric) latitude, which for the selected TAG site of Nightingale was -56.044 deg. The TAG sequence also required that ODM be located at a spacecraft phase angle of 91 ± 2 deg (3σ) and that the spacecraft be in a counterclockwise orbit when viewed from the Sun prior to orbit departure. Analysis of the current orbit leading up to TAG in early October 2020 showed that while the predicted range at ODM was 994 m, the predicted phase angle in the orbit at that time was 97.1 degrees, well outside of the defined specifications. The current spacecraft orbit, which was initiated following recovery from the second TAG Rehearsal at the end of August 2020, had slowly evolved away from the ideal frozen orbit conditions due to an imperfect orbit insertion, weekly desats, and imperfect modeling of the spacecraft attitude over the 8 weeks between orbit insertion and the TAG ODM. Thus, an orbit trim was required in order to correct the orbit prior to TAG. Given the above constraints, the targeted and achieved orbital elements for this trim are reported in Table 5, with the maneuver designs necessary to perform the trim included in Table 1. The semi-major axis and eccentricity were chosen to both satisfy the frozen orbit condition, while the true anomaly was selected to place the spacecraft at the proper latitude at the time of ODM for TAG on October 20, 2020. The values for i, Ω, and ω are slight modifications to the values listed in Table 4 to account for the perturbations due to J_2 and J_3, as well as other sources detailed in Ref. [10]. Finally, the target true anomaly was determined to minimize the potential ΔV of phasing burns leading up to TAG. Ideally, the orbit specified under 'Initial Target' in Table 5 would have arrived at the ODM latitude at the correct time without requiring any phasing maneuvers.

Table 5 – Pre-TAG Trim Targeted and Achieved Parameters

	Pre-Trim Orbit	Initial Target	Final Target	Achieved
a, m	910.07	905.15	884.82	905.33
e	0.17	0.15	0.18	0.16
i, deg	84.09	89.75	90.05	89.82
Ω, deg	269.63	269.76	269.51	269.80
ω, deg	77.77	91.11	94.44	89.98
θ, deg	254.35	218.32	207.41	213.67

The as-flown orbital elements for this orbit trim are shown in Fig. 5, starting from just after orbit insertion until shortly before departing orbit for TAG. The increasing trend in terminator angle is clearly observed, and the correction provided by the trim maneuver is obvious. While the trim execution did not eliminate the need for phasing maneuvers, it did help decrease their potential size, which in turn reduced possible delivery errors to the orbit departure point for TAG, as detailed in the next section.

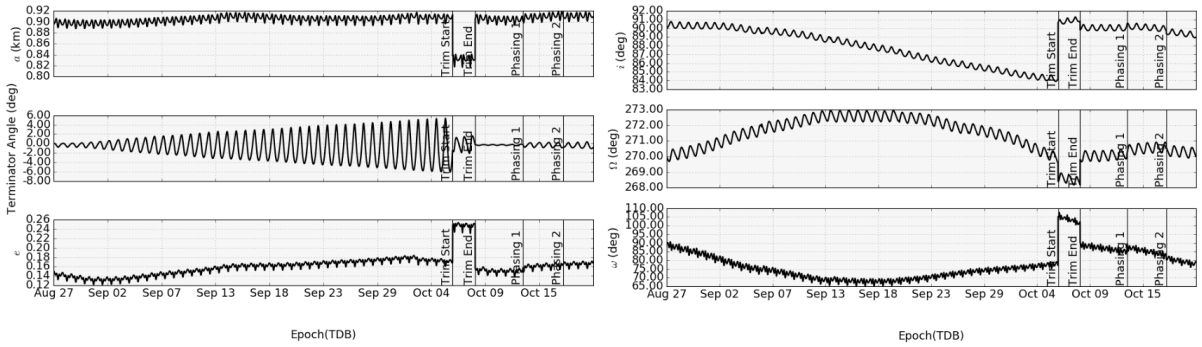

Fig. 5 As-flown pre-TAG orbital parameters in the SAM frame

VI. Phasing Maneuver Results

Phasing burns were critical in several phases in order to place the spacecraft at a specific point in orbit at a particular time. For the medium- and low-altitude Reconnaissance phases, the spacecraft had to depart orbit from a particular latitude relative to the site of interest, at the correct time such that the spacecraft was at a low altitude over the correct site with the proper lighting conditions. [12] In addition, the sortie across the surface had to be such that the orbit recapture maneuver (ORM) returned the spacecraft back to a safe, frozen orbit. In order to achieve all of these targeting conditions, the execution time of both ODM and ORM had to be variable, but could only be allowed within a specified window. Thus, execution of the phasing burns had to guarantee both maneuvers fit within the allotted window of ±40 minutes around the nominal time for each, in addition to maximizing the time that the spacecraft was within the defined science constraints for observing the sample site. [12]

A total of 4 reconnaissance sorties were performed: a medium and a low altitude sortie at both the prime sample site, Nightingale (56.044 deg latitude), and the backup site, Osprey (11.62 deg latitude). Each of these required only a single phasing maneuver except for the low sortie over Osprey, which required two. The 5 phasing maneuvers ranged in ΔV from 0.92 (Nightingale Low Sortie) to 3.84 mm/s (Osprey Low Sortie 2) as shown in Table 2, and were all performed using a 0.08 N thruster, the smallest on the spacecraft. The delivery results for each maneuver are shown in Table 6. The first sortie performed, medium altitude at Nightingale, aimed to depart orbit from a latitude of around 20 degrees, while others had to depart near the equator in order to achieve the necessary observing conditions. The last two columns in Table 6 show the timing error in minutes relative to the nominal execution time from the reference trajectory, with each shift lying within the ±40 minute limit after completing the phasing maneuver. While the first phasing maneuver for the low-altitude sortie at Osprey placed the ODM and ORM maneuver times within limits, the departure latitude of 11.40 deg was too high to relative to the site to meet the lighting conditions necessary for science, thus a second phasing maneuver was performed to correct this residual error.

Table 6 – Reconnaissance Phasing Maneuver Delivery Performance

		ODM Latitude deg	Radius @ ODM m	Phase Angle @ ODM deg	ODM Timing Error min	ORM Timing Error min
	Requirement	±6.00			±40.00	±40.00
Nightingale Medium Sortie	Pre-Phasing	5.63	1250.96	91.15	-98.00	-
	Final Design	18.74	1176.93	85.76	-0.65	-17.22
	Achieved	19.84	1179.08	85.72	2.01	-15.44
Osprey Medium Sortie	Pre-Phasing	60.70	1319.66	91.63	722.18	-
	Final Design	-0.90	1098.82	95.53	-37.29	3.17
	Achieved	-3.64	1096.90	95.44	-36.62	5.47
Nightingale Low Sortie	Pre-Phasing	54.99	1039.09	93.84	227.46	-
	Final Design	-0.06	957.39	90.83	-1.55	3.70
	Achieved	0.05	965.29	90.85	-2.25	3.99
Osprey Low Sortie 1	Pre-Phasing	-79.25	928.27	88.84	-304.12	-
	Final Design	0.00	1027.56	88.83	-1.11	-7.68
	Achieved	11.40	1054.31	89.15	-18.27	-13.89
Osprey Low Sortie 2	Final Design	0.29	977.29	90.06	0.07	-0.38
	Achieved	1.26	984.05	90.06	1.55	4.04

For TAG, the entire sequence ran on a strict timeline that began with orbit departure and ended with the spacecraft touching down on the surface at a particular local time of day. [8] Backing this up meant that the orbit departure burn, which occurred at the Bennu geocentric latitude opposite of the TAG site, was fixed in time and could not be adjusted like the Reconnaissance sorties. In order to aid in the convergence of the on-board optical navigation software used during the descent to the surface, the spacecraft had to be placed near the ideal ODM location, with the nominal target and allowable errors defined in the first row of Table 7.

Checkpoint Rehearsal, performed in April 2020, required two phasing maneuvers in order to deliver the spacecraft to the required area. The first phasing maneuver, CP Rehearsal 1, was performed a week in advance of ODM, and had a final design ΔV of 0.43 mm/s – nearly 50% smaller than any other maneuver to that point in the mission. At that low range the extent of the possible delivery errors is quite significant, and indeed the reconstruction of that maneuver showed a ΔV magnitude error of 2.7σ (see Table 2), leaving a residual 6.61±1.62 deg of latitude error from the desired -56.04 deg. This necessitated the execution of another phasing maneuver at 3 days prior to ODM. The final design of the second phasing maneuver showed a ΔV of just over 0.1 mm/s, much smaller even than the first. The team was concerned that such a small maneuver could significantly overburn and place the resulting ODM location outside of specifications, thus the team selected to undershoot the ODM target with a fixed delta-V magnitude of 0.09 mm/s. The performance of these maneuvers is included in Table 2, and the resulting delivery error is shown in Table 7, where the errors are represented as the differences from the requirements listed in the first row, along with the predicted 3σ errors. The rehearsal departed from a latitude of -53.80 deg, just short of the target but still well within the requirements.

Table 7 – TAG and TAG Rehearsal Phasing Maneuver Delivery Errors

		ODM Latitude Error		Radial Error @ ODM		Phase Angle Error @ ODM	
		deg	±3σ	m	±3σ	deg	±3σ
Delivery Requirements		-56.04	±6.00	1000.00	±50.00	91.00	±2.00
CP Rehearsal 1	Pre-Phasing	23.73	±3.45	12.31	±2.27	0.54	±0.09
	Final Design	0.00	±7.56	-7.23	±10.78	-0.11	±0.16
	Achieved	6.61	±1.62	-19.01	±3.52	-0.41	±0.07
CP Rehearsal 2	Final Design	2.82	±4.72	-9.40	±9.69	-0.21	±0.08
	Achieved	2.24		-6.90		-0.19	
MP Rehearsal	Pre-Phasing	23.32	±4.16	74.99	±9.97	0.89	±0.11
	Final Design	0.00	±18.07	0.00	±10.99	0.00	±0.27
	Achieved	2.66		-4.10		0.29	
TAG 1	Pre-Phasing	16.12	±5.27	-3.80	±13.80	-0.51	±0.11
	Final Design	0.00	±4.79	3.60	±11.5	-0.75	±0.11
	Achieved	-2.42	±1.06	9.00	±3.30	-0.61	±0.07
TAG 2	Final Design	1.50	±1.45	-5.50	±4.86	-0.25	±0.11
	Achieved	1.59		-5.97		-0.19	
	Achieved*	0.09		-0.47		0.06	

***TAG 2 target was biased from center of delivery requirement to attempt to match conditions from both rehearsals. These errors are relative to that target.**

Prior to Matchpoint Rehearsal, which was executed in August 2020, the spacecraft was in an orbit that was slightly too small, in addition to not being phased correctly to arrive at the ODM latitude at the correct time. This ended up being beneficial since it required the phasing burn to be slightly larger than what was observed with Checkpoint Rehearsal. The final design of the phasing burn, performed 7 days prior to ODM, had a design ΔV of 6.2 mm/s and successfully placed the spacecraft within the desired ODM bounds with just a single maneuver. Indeed, performance of this maneuver as shown in Table 2 was considerably better than the small phasing maneuvers prior to Checkpoint Rehearsal. Fortuitously the MP Rehearsal ODM latitude was within 0.2 deg of that seen in CP Rehearsal, which provided key repeatability for the flight system between the two rehearsals. The delivery results for the MP Rehearsal phasing maneuver are captured in Table 7.

As mentioned in the previous section, the pre-TAG orbit trim maneuver was designed in such a way to attempt to minimize the need for a phasing maneuver. Naturally, execution was not perfect and as such required a least one phasing maneuver, although the initial latitude error was smaller than either of the rehearsals. In an attempt to prevent larger delivery errors as seen in Checkpoint Rehearsal, the ΔV of the first phasing maneuver was fixed at 1 mm/s and the pointing of the maneuver was adjusted such that the ODM latitude was achieved. Naturally, this means that all

three target values could not be achieved, which is why the 'Final Design' row for TAG 1 in Table 7 are not all zeros. The maneuver performance was superb and the resulting trajectory satisfied all requirements. Upon reviewing the reconstructed trajectory prior to determining the need for a second phasing burn, the team had a concern that the ODM latitude would be lower than the nominal and either of the rehearsals. The team then elected to perform a second trim maneuver for TAG, but opted for it to target an ODM latitude similar to that seen in both of the Rehearsals as opposed to the original target of -56.044 deg. This final phasing maneuver had a ΔV of 0.5 mm/s and performed exceptionally well, as seen in the last rows of Tables 2 and 7 for maneuver execution performance and delivery error, respectively. The resulting changes to the spacecraft trajectory during this period can be seen near the end of the trajectory shown in Figure 5. The small adjustments are easier to see with the first maneuver due to its larger size, while the second phasing burn was a very small adjustment. Compared to both the nominal and the adjusted targets, all requirements were fully satisfied and helped lead to a successful sample collection.

VII. Conclusion

OSIRIS-REx spent a majority of the nearly 2 years of proximity operations near Bennu in orbit around the small asteroid. With so much time spent in this regime, the team needed a common strategy across all orbit designs and mission phases to plan any orbit adjustments that might be necessary. While the stability of the frozen orbit design required only a handful of orbit trims, the robust, consistent methodology for planning and performing these orbit trims proved to be vital to the mission's success. Using only a portion of the framework also proved critical in designing and performing phasing maneuvers to correctly place the spacecraft at the start of the sequences that ultimately brought the spacecraft to safely touch down on the asteroid's surface and collect a substantial sample of pristine asteroid regolith. The performance of these phasing maneuvers, some of which were exceedingly small, is yet another testament to the continuing outstanding performance of the OSIRIS-REx spacecraft. Notably, the described strategy can be applied to any future mission designs that include close proximity operations at a small body, with perhaps minimal adjustment to the schedule based on mission objectives and the chosen target body.

Acknowledgments

The authors acknowledge members of the OSIRIS-REx team who have contributed to the accomplishments described in this paper: members of the OpNav and Orbit Determination teams, led by Coralie Adam and Jason Leonard, respectively; the Lockheed Martin flight operations team with special emphasis on support from Ryan Olds and the Guidance, Navigation, and Control team, Carey Parish and the Propulsion team, and Olivia Billet and the Spacecraft Systems team; and members of the Science Planning and Science Operations teams at the University of Arizona who have supported OpNav observation planning.

This material is based upon work supported by NASA under Contracts NNM10AA11C and NNG13FC02C. OSIRIS-REx is the third mission in NASA's New Frontiers Program. Dante Lauretta of the University of Arizona, Tucson, is the mission's Principal Investigator, and the University of Arizona also leads the Science Team and the science observation planning and data processing. Lockheed Martin Space Systems in Denver built the spacecraft and is providing flight operations. Goddard Space Flight Center and KinetX Aerospace are responsible for navigating the OSIRIS-REx spacecraft. Contract NNM10AA11C is issued through the New Frontiers Program.

References

[1] Lauretta, D., et al, "OSIRIS-REx: Sample Return from Asteroid (101955) Bennu", *Space Science Reviews*, Vol. 212, 2017, pp. 925-984.

[2] Lauretta, D., Bartels, A., Barucci, M., Bierhaus, E., Binzel, R., Bottke, W., Campins, H., Chesley, S., Clark, B., Clark, B., et al., "The OSIRIS-REx target asteroid (101955) Bennu: Constraints on its physical, geological, and dynamical nature from astronomical observations," Meteoritics & Planetary Science, Vol. 50, No. 4, 2015, pp. 834–849.

[3] Wibben D.R., Levine A., Rieger, S., McAdams, J., Antreasian, P., Leonard, J.M., Moreau, M.C., and Lauretta, D., "OSIRIS-REx Navigation Campaign Trajectory Design and Maneuver Performance", *Proceedings of the 2019 AAS/AIAA Astrodynamics Specialist Conference*, AAS 19-676, 2019.

[4] Wibben, D.R., Levine, A., Rieger, S., McAdams, J., Getzandanner, K., Antreasian, P., Leonard, J., Moreau, M., and Lauretta, D.S., "Trajectory Design and Maneuver Performance of the OSIRIS-REx Detailed Survey of Bennu", *Proceedings of the 43rd Annual GN&C Conference*, 2020, AAS 20-151.

[5] Daly, MG., Barnouin, OS., Dickinson, C., Seabrook, J., Johnson, CL., Cunningham, G., Haltigin, T., Gaudreau, D., Brunet, C., and Aslam, I, "The OSIRIS-REx laser altimeter (OLA) investigation and instrument", *Space Science Reviews*, Vol. 212, No. 1, 2017, pp. 899-924.

[6] Seabrook, J. A., et al. "Global shape modeling using the OSIRIS-REx scanning Laser Altimeter." Planetary and Space Science 177 (2019): 104688.

[7] Lauretta, D., Enos, H., Polit, A., Roper, H. and Wolner, C., "OSIRIS-REx at Bennu: Overcoming challenges to collect a sample of the early Solar System", *Sample Return Missions*, 2021, pp.163-194.

[8] Berry, K., Getzandanner, K., Moreau, M., Rieger, S., Antreasian, P., Adam, C., Wibben, D., Leonard, J., Levine, A., Geeraert, J., Lorenz, D., and Lauretta, D.S., "Contact with Bennu! Flight Performance versus prediction of OSIRIS-REx "TAG" Sample Collection", *Proceedings of the 2022 AAS/AIAA Space Flight Mechanics Meeting*, 2022.

[9] Scheeres, D., "Satellite Dynamics about Small Bodies: Averaged Solar Radiation Pressure Effects", *Journal of the Astronautical Sciences*, Vol. 47, No. 1, 1999, pp. 25-46.

[10] Wibben D.R., Levine A., Rieger, S., McAdams, J., Antreasian, P., Leonard, J.M., Moreau, M.C., and Lauretta, D., "OSIRIS-REx Frozen Orbit Design and Flight Experience", *Proceedings of the 2019 AAS/AIAA Astrodynamics Specialist Conference*, AAS 19-677, 2019.

[11] Lauretta, D., Hergenrother, C., Chesley, S., Leonard, J., et al., "Episodes of particle ejection from the surface of the active asteroid (101955) Bennu", *Science*, Vol. 366, No. 6470, 2019.

[12] Levine, A., Wibben, D.R., Rieger, S., McAdams, J.V., Antreasian, P., Getzandanner, K., Moreau, M., and Lauretta, D.S., "Trajectory Design and Maneuver Performance of the OSIRIS-REx Low Altitude Reconnaissance of Bennu", *Proceedings of the 2022 AAS/AIAA Space Flight Mechanics Meeting*, 2022.

[13] Leonard, J., Geeraert, J., Pelgrift, J., Antreasian, A., Adam, C., Wibben, D.R., Getzandanner, K., Ashman, B., Lauretta, D.S., "Navigation Prediction Performance During the OSIRIS-REx Proximity Operations at (101955) Bennu", *Proceedings of the 2022 AAS/AIAA Space Flight Mechanics Meeting*, 2022.

[14] Antreasian, P., Adam, C., Berry, K., Geeraert, J., Getzandanner, K., Highsmith, D., Leonard, J., Lessac-Chenen, E., Levine, A., McAdams, J., McCarthy, L., Moreau, M., Nelson, D., Page, B., Pelgrift, J., Rieger, S., Sahr, E., Wibben, D., Williams, B., Williams, K., Lauretta, D.S., "OSIRIS-REx Proximity Operations and Navigation Performance at Bennu", *Proceedings of the 2022 AAS/AIAA Space Flight Mechanics Meeting*, 2022.

[15] Rosengren, A., Scheeres, D., "On the Milankovitch orbital elements for perturbed Keplerian motion", *Celestial Mechanics and Dynamical Astronomy*, Vol 118, pp. 197-220, 2014.